LIQUID CRYSTALS, 2002, VOL. 29, NO. 9, 1121–1132

Taylor & Francis
Taylor & Francis Group

Synthesis and thermal behaviour of liquid crystalline pyridinium bromides containing a biphenyl core

LI CUI, VYTENIS SAPAGOVAS and GÜNTER LATTERMANN*
Makromolekulare Chemie I, Universität Bayreuth, D-95440 Bayreuth, Germany

(*Received 3 December 2001; in final form 26 March 2002; accepted 8 April 2002*)

A range of new pyridinium bromides was synthesized by the quaternization of different substituted pyridines with a group containing a biphenyl core and alkyl chains of differing lengths. The phase behaviour of the pyridinium bromides was studied by differential scanning calorimetry, polarizing optical microscopy and powder X-ray diffraction. It is shown that pyridinium moieties, linked to a rod-like biphenyl core via an alkyl spacer, can form ionic liquid crystals. Unsubstituted pyridinium groups promote mesomorphism. Liquid crystalline phases are formed only from 2- and 4-ethyl substituted pyridinium groups with sufficiently long alkyl terminal chains and spacers; i.e. decyl chains on both sides of the biphenyl core. Both the substitution pattern at the pyridinium group and the alkyl chain length have an influence on the polymorphism of the smectic phases. 3,5-Dimethyl substitution hinders mesophase formation.

1. Introduction

In recent years, the interest in ionic liquid crystals has grown considerably. Ion conductivity in mesophases, self assembled wires and channels has been investigated [1–4]. Furthermore, ionic liquid crystals with relatively low melting points have been described as ordered solvents for polymerizations [5] and stereochemically controlled organic reactions [6]. In general, various classes of low molar mass ionic liquid crystals are known. In addition to liquid crystalline alkali and alkaline earth alkanoates, the majority of mesogenic metal complexes exhibit ionic character. This area has been extensively reviewed [1, 7, 8].

In this group of ionic liquid crystals, those containing nitrogen comprise, besides alkylammonium compounds with metallic cations [1, 9], a large number of metal complexes with macrocyclic ligands [10] such as phthalocyanines [1] or azacycles [11–14], with linear [15–17], branched or dendrimeric [18, 19] amine ligands, or with pyridine ligands [20–22]. On the other hand, numerous low molar mass liquid crystalline, linear [23–30], branched, dendrimeric [31] or cyclic [32], protonated or quaternized ammonium compounds have been reported. Furthermore, besides vinamidinium ionic mesogens [33], various liquid crystalline heteroaromatic salts such as aryl pyrylium, thiopyrylium and dithiopyrylium ionic liquid crystals have been described [34–36]. Finally, to this group of heteroaromatic ionic liquid crystals belong alkyl-substituted pyridinium salts [37–54] and derivatives thereof [55–58]. Instead of quaternizing only with alkyl chains, anisometric mesogenic units, i.e. rod-like groups, have also been attached to the pyridine moiety via spacers [59–62]. Recently, the formation of hydrogen-bonded ionic associates of carboxylic acids or phenols and (4-pyridyl)pyridinium compounds was achieved [63].

Most ionic liquid crystals form smectic mesophases, except for several columnar ionic metal complexes. With respect to pyridinium derivatives, many investigations were performed on the influence of the spacer length on the mesophase behaviour, and not on the substitution pattern of the pyridinium moiety. Only in one report [50], is substitution in the 3- and 4-positions of *N*-alkylated pyridinium salts described, and this decreases the melting point as well as the tendency to exhibit mesomorphism. We wanted to know if this relationship also applies to liquid crystalline pyridinium salts with an attached conventional, anisometric mesogenic unit. Therefore, we synthesized a series of low molar mass pyridinium bromides by the quaternization of different substituted pyridines with a group containing a biphenyl core and studied their phase behaviour.

2. Experimental

2.1. *Methods of characterization*

^{1}H NMR spectra were recorded on a Bruker spectrometer (250 MHz, AC 250) using $CDCl_3$ solutions with an internal TMS standard. IR spectra were recorded

*Author for correspondence;
e-mail: guenter.lattermann@uni-bayreuth.de

Liquid Crystals ISSN 0267-8292 print/ISSN 1366-5855 online © 2002 Taylor & Francis Ltd
http://www.tandf.co.uk/journals
DOI: 10.1080/02678290210155589

with a BioRad Digilab FTS-40 FTIR spectrometer using pellets of ~1 mg sample dispersed in ~200 mg potassium bromide. Elemental analysis (EA) was performed by Ilse Beetz, Mikroanalytisches Laboratorium, D-96301 Kronach. The thermal behaviour was observed with a Nikon Diaphot 300 polarizing optical microscope (POM) equipped with a Mettler FP 82 hot stage and FP 80 processing unit. Transition temperatures and enthalpies were recorded with a Perkin Elmer DSC 7 differential scanning calorimeter (heating and cooling rate 10 K min^{-1}). Thermogravimetrical measurements (TGA) were performed on a Netzsch Simultan TGA STA 409 C. Powder X-ray diffraction (XRD) was carried out with a Huber Guinier goniometer 600 system, including a Huber quartz monochromator 611 and a copper anode (CuK_{α_1} radiation, $\lambda = 0.154$ nm). The system was equipped with a Seifert X-ray generator, a Huber HTC 9000 stepping motor controller, a Huber HTC 9634 temperature controller and self-constructed components such as a slit system, a primary beam stop and sample oven ($\Delta T = \pm 0.2$ K). The samples were prepared on a steel grid; lead nitrate was used for calibration.

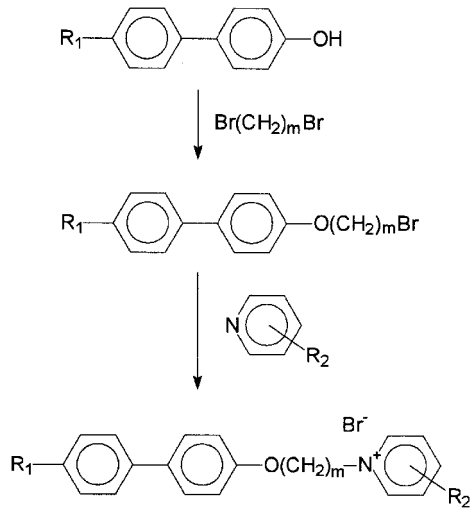

R_1 = CN, $O(CH_2)_2CH_3$, $O(CH_2)_9CH_3$

R_2 = H, 4-ethyl, 2-ethyl, 3,5-dimethyl

m = 6, 10

Scheme 1. Synthetic scheme for the pyridinium salts.

2.2. *Materials and synthesis*

All solvents were distilled before use. Argon was dried and purified by passing through columns containing molecular sieves (3 Å) and subsequently, potassium dispersed on aluminium oxide powder. Pyridine, 4-ethylpyridine, 2-ethylpyridine and 3,5-dimethylpyridine were distilled over potassium hydroxide before use. All other chemicals were used without further purification.

The synthetic route to the pyridinium salts is shown in scheme 1. The purity of the products was characterized by thin layer chromatography (TLC), gel permeation chromatography (GPC), and in the case of the liquid crystalline pyridinium products, by elemental analysis (EA). Structural characterization of the products was made by FTIR, and ^{1}H NMR spectroscopy, thermal characterization by POM, DSC and TGA, and mesophase characterization by XRD.

2.2.1. *4-Hydroxy-4′-alkoxybiphenyl compounds*

These were synthesized by a classical method using 4,4′-dihydroxybiphenyl (Aldrich) and alkyl bromides. Thus, as a general example, the synthesis of 4-hydroxy-4′-propyloxybiphenyl is described [64]. In a 500 ml flask, 18.6 g (0.1 mol) of 4,4′-dihydroxybiphen yl, 27.6 g (0.2 mol) of finely powdered potassium carbonate (K_2CO_3), 0.5 g of potassium iodide (KI, Aldrich) and 150 ml of acetone were placed; the mixture was stirred and heated to reflux. An acetone solution, containing 12.3 g (0.1 mol) of 1-bromopropane was added dropwise, and the suspension stirred for a further 18 h under reflux. The reaction mixture was filtered and the solid residue washed with THF (3 × 40 ml). The remaining THF solution was combined with the former filtrate and the solvent evaporated under reduced pressure. The residue was dissolved in hot ethanol from which the side product 4,4′-dipropyloxybiphenyl precipitated on cooling. From the concentrated mother solution, the crude product was crystallized. After further recrystallization twice from ethyl acetate, the pure 4-hydroxy-4′-propyloxybiphenyl was obtained. Yield: 34%, needle-like crystals, m.p. 171–172°C. ^{1}H NMR (δ, $CDCl_3$): 1.05 (t, 3H, $C\underline{H}_3CH_2$), 1.82 (m, 2H, $CH_3C\underline{H}_2$), 3.98 (t, 2H, CH_2O), 4.69 (s, 1H, OH), 6.9 (m, 4H, ArH), 7.44 (m, 4H, ArH). FTIR, KBr (cm^{-1}): 3370, 2964, 2925, 2873, 1883, 1611, 1597, 1500, 1477, 1450, 1378, 1309, 1244, 1194, 1177, 1134, 1069, 1024, 979, 919, 885, 815, 759, 706, 683, 569, 515.

The side product, 4,4′-dipropyloxybiphenyl [65], was recrystallized from ethanol. Yield: 24%, plate-like crystals, m.p. 158–159°C. ^{1}H NMR (δ, $CDCl_3$): 1.05 (t, 6H, $C\underline{H}_3CH_2$), 1.82 (m, 4H, $CH_3C\underline{H}_2$), 3.95 (t, 4H, CH_2O), 6.92 (m, 4H, ArH), 7.44 (m, 4H, ArH). FTIR, KBr (cm^{-1}): 3040, 2964, 2933, 2875, 1889, 1606, 1568, 1498, 1471, 1393, 1328, 1269, 1237, 1179, 1138, 1069, 1033, 974, 823, 808, 645, 592, 517.

2.2.2. *4-(ω-Bromoalkoxy)-4′-alkyloxybiphenyl and 4-(6-bromohexyloxy)-4′-cyanobiphenyl*

These were synthesised by the reaction of α,ω-dibromoalkanes with 4-hydroxy-4′-alkoxybiphenyl or 4-hydroxy-4′-cyanobiphe nyl, respectively. As a representative example,

the synthesis of 4-(6-bromohexyloxy)-4′-propyloxybiphenyl is described. Thus, in a 250 ml flask, 16.6 g (0.068 mol) of 1,6-dibromohexane, 19.3 g (0.14 mol) of finely powdered potassium carbonate, 0.2 g of potassium iodide and 100 ml of cyclohexanone were placed. The mixture was stirred and heated to 100°C. A cyclohexanone solution containing 7.76 g (0.034 mol) of 4′-hydroxy-4-propyloxybiphenyl was then added dropwise, and the suspension stirred for a further 20 h at 100°C. The reaction mixture was filtered to separate the inorganic salts; from the filtrate, the solvent was removed under reduced pressure. The residue was washed with cold methanol and recrystallized from ethanol. Yield: 50%, plate-like white crystals, m.p. 116–117°C. ^{1}H NMR (δ, $CDCl_3$): 1.05 (t, 3H, $C\underline{H}_3CH_2$), 1.55 (m, 4H, $C\underline{H}_2C\underline{H}_2CH_2CH_2Br$), 1.75–2.0 (t, 6H, $C\underline{H}_2CH_2CH_2C\underline{H}_2CH_2Br$ and $CH_3C\underline{H}_2$), 3.44 (t, 2H, CH_2Br), 3.95 (m, 4H, OCH_2), 6.94 (m, 4H, ArH), 7.46 (m, 4H, ArH). FTIR, KBr (cm^{-1}): 2964, 2938, 2864, 1607, 1569, 1501, 1475, 1394, 1273, 1248, 1179, 1035, 996, 977, 824, 809, 648, 593, 519.

4-(10-Bromodecyloxy)-4′-propyloxybiphenyl: yield 58%, plate-like white crystals, m.p. 107–108°C. ^{1}H NMR (δ, $CDCl_3$) and FTIR, KBr (cm^{-1}): equivalent to 4-(6-bromohexyloxy)-4′-propyloxybiphenyl. *4-(10-Bromodecyloxy)-4′-decyloxybiphenyl*: yield 63%, plate-like white crystals, m.p. 106–107°C. ^{1}H NMR (δ, $CDCl_3$): 0.88 (t, 3H, CH_3), 1.28 (m, 20H, $OCH_2CH_2CH_2(C\underline{H}_2)_6$ and $C\underline{H}_2)_4CH_2CH_2CH_2Br$), 1.43 (m, 6H, $C\underline{H}_2CH_2CH_2O$ and $C\underline{H}_2CH_2CH_2Br$), 1.81 (m, 6H, $C\underline{H}_2CH_2O$ and $C\underline{H}_2CH_2Br$), 3.41 (t, 2H, CH_2Br), 3.98 (t, 4H, CH_2O), 6.94 (d, 4H, ArH), 7.45 (d, 4H, ArH). FTIR, KBr (cm^{-1}): equivalent to 4-(6-bromohexyloxy)-4′-propyloxybiphenyl. *4-(6-Bromohexyloxy)-4′-cyanobiphenyl* [66]: yield 64.2%, needle like white crystals, m.p. 66°C (monotropic LC). ^{1}H NMR (δ $CDCl_3$): 1.5 (m, 4H, $OCH_2CH_2(C\underline{H}_2)_2$), 1.9 (m, 4H, $OCH_2C\underline{H}_2$ and $C\underline{H}_2CH_2Br$), 3.44 (t, 2H, CH_2Br), 4.04 (t, 2H, OCH_2), 7.0 (m, 2H, ArH), 7.5 (m, 2H, ArH), 7.65 (m, 4H, ArH). FTIR, KBr (cm^{-1}): 2936, 2921, 2857, 2226, 1600, 1578, 1529, 1494, 1469, 1388, 1288, 1267, 1249, 1215, 1200, 1182, 1076, 1052, 981, 912, 818, 659, 644, 558, 529.

2.2.3. *Pyridinium salts*

These were obtained by reacting the bromo-substituted compounds with pyridine derivatives of different substitution patterns (cf. scheme 1). As an example, the general synthesis of 1-[6-(4′-propyloxyl-4-biphenylyloxy)-hexyl]pyridinium bromides is described. In a round flask, 391 mg (0.001 mol) of 4-(6-bromohexyloxy)-4′-propyloxybiphenyl was added with 10 ml of the pyridine derivative. The reaction was carried out under argon and monitored by TLC using $CHCl_3$/acetone as eluent (1/1). When starting materials were no longer detected, the reaction mixture was placed in the freezer (~ -20°C). The crystallized product was filtered off and washed with cold diethyl ether to remove non-reacted reagents. The product was recrystallized to purity from a mixture of ethyl acetate/ethanol (10/1) and dried at 60°C under vacuum. The resulting quaternized products are in general somewhat hygroscopic and were therefore kept under dry inert gas. Preparations for measurements of elemental analysis, transition temperatures, etc. were done quickly enough to avoid water absorption.

Yields, melting points and degradation onset temperatures of the pyridinium salts are summarized in table 1.

Table 1. Synthetic data for the pyridinium salts.

No.	Pyridinium derivative	Yield/%	Melting point/°C	Degradation onset/°C
1	CNBpOC6-Py	56	LC	213
2	CNBpOC6-(4-Et)Py	79	67–69	
3	CNBpOC6-(2-Et)Py	48	99–101	
4	CNBpOC6-(3,5-Me)Py	66	143–144	
5	C3OBpOC6-Py	78	LC	204
6	C3OBpOC6-(4-Et)Py	91	116–117	
7	C3OBpOC6-(2-Et)Py	57	120–121	
8	C3OBpOC6-(3,5-Me)Py	72	165–166	
9	C3OBpOC10-Py	72	LC	205
10	C3OBpOC10-(4-Et)Py	93	117–119	
11	C3OBpOC10-(2-Et)Py	69	139–141	
12	C3OBpOC10-(3,5-Me)Py	97	130–131	
13	C10OBpOC10-Py	68	LC	205
14	C10OBpOC10-(4-Et)Py	62	LC	203
15	C10OBpOC10-(2-Et)Py	62	LC	193
16	C10OBpOC10-(3,5-Me)Py	83	143–144	

2.2.3.1. *1-[6-(4′-Cyano-4-biphenyl loxy)hexyl]-pyridinium bromide; $R_1 = CN$, $m = 6$, $R_2 = H$; CNBpOC6-Py,* ***1***. The reaction was carried out in an analogous fashion to the general synthesis at 45–55°C for 20 h. The product was recrystallized from acetonitrile and dried at 70°C under vacuum. Yield: 56%, white crystals, monotropic liquid crystalline. ^{1}H NMR (δ, $CDCl_3$): 1.54 (m, 4H, $OCH_2CH_2C\underline{H}_2C\underline{H}_2$), 1.79 (p, 2H, $OCH_2C\underline{H}_2$), 2.11 (p, 2H, $C\underline{H}_2CH_2N^+$), 3.99 (t, 2H, OCH_2), 5.10 (t, 2H, CH_2N^+), 6.95 (d, 2H, ArH), 7.49 (d, 2H, ArH), 7.65 (m, 4H, ArH), 8.12 (t, 2H, β-PyH), 8.51 (t, 1H, γ-PyH), 9.60 (d, 2H, α-PyH). FTIR, KBr (cm^{-1}): 3445, 3053, 2941, 2864, 2227, 1638, 1603, 1577, 1495, 1473, 1396, 1314, 1294, 1271, 1255, 1176, 1060, 1039, 996, 868, 852, 822, 791, 736, 691, 528, 489. EA for $C_{24}H_{25}N_2OBr$: calcd H 5.76, C 65.91, N 6.40, Br 18.27; found H 5.70, C 65.10, N 5.87, Br 17.45%.

2.2.3.2. *1-[6-(4′-Cyano-4-biphenylyloxy)hexyl]-4-ethyl-pyridinium bromide; $R_1 = CN$, $m = 6$, $R_2 = 4$-Et; CNBpOC6-(4-Et)Py,* ***2***. The reaction was carried out as before, at 45–55°C for 20 h. The product was recrystallized from acetone and dried at 50°C under vacuum. Yield: 79%, pale white crystals, m.p. 67–69°C. ^{1}H NMR (δ, $CDCl_3$): 1.35 (t, 3H, $C\underline{H}_3CH_2Py$), 1.52 (m, 4H, $OCH_2CH_2C\underline{H}_2C\underline{H}_2$), 1.77 (p, 2H, $OCH_2C\underline{H}_2$), 2.08 (p, 2H, $C\underline{H}_2CH_2N^+$), 2.93 (q, 2H, CH_2Py), 3.98 (t, 2H, OCH_2), 5.00 (t, 2H, CH_2N^+), 6.96 (d, 2H, ArH), 7.51 (d, 2H, ArH), 7.65 (m, 4H, ArH), 7.85 (d, 2H, β-PyH), 9.42 (d, 2H, α-PyH). FTIR, KBr (cm^{-1}): 3408, 3016, 2972, 2937, 2871, 2220, 1639, 1599, 1520, 1494, 1474, 1400, 1314, 1291, 1249, 1178, 1036, 997, 860, 836, 829, 796, 730, 660, 532.

2.2.3.3. *1-[6-(4′-Cyano-4-biphenylyloxy)hexyl]-2-ethyl-pyridinium bromide; $R_1 = CN$, $m = 6$, $R_2 = 2$-Et; CNBpOC6-(2-Et)Py,* ***3***. The reaction was carried out as before at 70°C for 6 days. The product was recrystallized from acetone. Yield: 48%, slightly yellow crystals, m.p. 99–101°C. ^{1}H NMR (δ, $CDCl_3$): 1.50 (t, 3H, $C\underline{H}_3CH_2Py$), 1.60 (m, 4H, $OCH_2CH_2C\underline{H}_2C\underline{H}_2$), 1.83 (p, 2H, $OCH_2C\underline{H}_2$), 2.03 (p, 2H, $C\underline{H}_2CH_2N^+$), 3.22 (q, 2H, CH_2Py), 4.01 (t, 2H, OCH_2), 5.01 (t, 2H, CH_2N^+), 6.98 (d, 2H, ArH), 7.52 (d, 2H, ArH), 7.66 (m, 4H, ArH), 7.87 (d, 1H, β-PyH), 7.99 (t, 1H, β-PyH), 8.43 (t, 1H, γ-PyH), 9.98 (d, 1H, α-PyH). FTIR, KBr (cm^{-1}): 3435, 3036, 2940, 2866, 2226, 1631, 1603, 1578, 1516, 1496, 1474, 1398, 1314, 1291, 1269, 1256, 1177, 1060, 1035, 996, 821, 792, 656, 529.

2.2.3.4. *1-[6-(4′-Cyano-4-biphenylyloxy)hexyl]-3,5-dimethylpyridinium bromide; $R_1 = CN$, $m = 6$, $R_2 = 3,5$-Me; CNBpOC6-(3,5-Me)Py,* ***4***. The reaction was carried out as before, at 45–55°C for 20 h. The product was recrystallized from acetonitrile/acetone (2/3 v/v). Yield: 66%, pale white crystals, m.p. 143–144°C. ^{1}H NMR (δ, $CDCl_3$): 1.53 m, 4H, $OCH_2CH_2C\underline{H}_2C\underline{H}_2$), 1.80 (p, 2H, $OCH_2C\underline{H}_2$), 2.10 (p, 2H, $C\underline{H}_2CH_2N^+$), 2.59 (q, 6H, CH_3Py), 3.99 (t, 2H, OCH_2), 4.96 (t, 2H, CH_2N^+), 6.96 (d, 2H, ArH), 7.48 (d, 2H, ArH), 7.62 (m, 4H, ArH), 7.98 (s, 1H, γ-PyH), 9.26 (s, 2H, α-PyH). FTIR, KBr (cm^{-1}): 3422, 3001, 2933, 2861, 2222, 1601, 1522, 1494, 1465, 1395, 1292, 1249, 1176, 1030, 1012, 829, 803, 794, 697, 568, 534.

2.2.3.5. *1-[6-(4′-Propyloxyl-4-biphenylyloxy)hexyl]-pyridinium bromide; $R_1 = O(CH_2)_3H$, $m = 6$, $R_2 = H$; C3OBpOC6-Py,* ***5***. The reaction was carried out as before, at 80°C for 27 h. The product was recrystallized from 10 ml of ethyl acetate with a few drops of ethanol, and dried at 60°C under vacuum. Yield: 64%, white crystals, liquid crystalline. ^{1}H NMR (δ, $CDCl_3$): 1.05 (t, 3H, CH_3), 1.4–1.6 (m, 4H, $C\underline{H}_2C\underline{H}_2CH_2CH_2N^+$), 1.7–1.9 (m, 2H, $C\underline{H}_2CH_2O$), 2.02–2.18 (m, 4H, $C\underline{H}_2CH_2N^+$), 3.97 (m, 4H, CH_2O), 5.05 (t, 2H, CH_2N^+), 6.92 (t, 4H, ArH), 7.45 (d, 4H, ArH), 8.05 (t, 2H, β-PyH), 8.42 (t, 1H, γ-PyH), 9.5 (d, 2H, α-PyH). FTIR KBr, (cm^{-1}): 3422, 3039, 2936, 2870, 1634, 1606, 1501, 1394, 1328, 1273, 1249, 1179, 1034, 976, 824, 808, 775, 686, 591, 518. EA for $C_{26}H_{32}NO_2Br$: calcd H 6.86, C 66.38, N 2.98, Br 16.98; found H 6.88, C 65.87, N 2.77, Br 15.70%.

2.2.3.6. *1-[6-(4′-Propyloxyl-4-biphenylyloxy)hexyl]-4-ethyl-pyridinium bromide; $R_1 = O(CH_2)_3H$, $m = 6$, $R_2 = 4$-Et; C3OBpOC6-(4-Et)Py,* ***6***. The reaction was carried out as before, at 50°C for 40 h. The final reaction mixture was washed with cold diethyl ether with stirring, and the final filtered product was dried at 50°C under vacuum. Yield: 90%, pale white powder, m.p. 116–117°C. ^{1}H NMR (δ, $CDCl_3$): 1.05 (t, 3H, CH_3), 1.35 (t, 3H, $PyCH_2C\underline{H}_3$), 1.4–1.65 (m, 4H, $C\underline{H}_2C\underline{H}_2CH_2CH_2N^+$), 1.72–1.95 (m, 4H, $C\underline{H}_2CH_2O$), 1.95–2.2 (m, 2H, $C\underline{H}_2CH_2N^+$), 3.05 (m, 2H, $PyCH_2$), 3.95 (m, 4H, CH_2O), 5.0 (t, 2H, CH_2N^+), 6.94 (t, 4H, ArH), 7.45 (d, 4H, ArH), 7.8 (d, 2H, β-PyH), 9.3 (d, 2H, α-PyH). FTIR, KBr (cm^{-1}): 3421, 2936, 2872, 1640, 1607, 1501, 1472, 1394, 1273, 1249, 1180, 1050, 977, 825, 808, 518.

2.2.3.7. *1-[6-(4′-Propyloxyl-4-biphenylyloxy)hexyl]-2-ethyl-pyridinium bromide; $R_1 = O(CH_2)_3H$, $m = 6$, $R_2 = 2$-Et; C3OBpOC6-(2-Et)Py,* ***7***. The reaction was carried out as before, at 80°C for 6 days. The product was recrystallized from 15 ml of ethyl acetate with a small amount of ethanol. Yield: 57%, light yellow solid, m.p. 120–121°C. ^{1}H NMR (δ, $CDCl_3$): 1.08 (t, 3H, CH_3), 1.5 (t, 3H, $PyCH_2C\underline{H}_3$), 1.5–1.7 (m, 4H, $C\underline{H}_2C\underline{H}_2CH_2CH_2N^+$), 1.72–1.92 (m, 4H, $C\underline{H}_2CH_2O$), 1.92–2.2 (m, 2H, $C\underline{H}_2CH_2N^+$), 3.2 (m, 2H, CH_2Py), 3.98 (m, 4H, CH_2O), 5.02 (t, 2H, CH_2N^+), 6.9 (t, 4H, ArH), 7.45 (d, 4H, ArH), 7.78 (d, 1H, β-PyH), 7.98 (t, 1H, β-PyH), 8.35

(t, 1H, γ-PyH), 9.9 (d, 1H, α-PyH). FTIR, KBr (cm^{-1}): 3421, 3039, 2936, 2872, 1629, 1607, 1501, 1473, 1394, 1272, 1249, 1179, 1033, 977, 824, 808, 596, 518.

2.2.3.8. *1-[6-(4′-Propyloxyl-4-biphenylyloxy)hexyl]-3,5-dimethylpyridinium bromide;* $R_1 = O(CH_2)_3H$, $m = 6$, $R_2 = 3,5\text{-}Me$; *C3OBpOC6-(3,5-Me)Py,* ***8***. The reaction was carried out as before, at 100°C for 20 h. The final reaction mixture was washed with cold diethyl ether and dried at 50°C under vacuum. Yield: 72%, pale white solid, m.p. 165–166°C. ^{1}H NMR (δ, $CDCl_3$): 1.05 (t, 3H, CH_3), 1.4–1.6 (m, 4H, $C\underline{H}_2C\underline{H}_2CH_2CH_2N^+$), 1.7–1.9 (m, 4H, $C\underline{H}_2CH_2O$), 2.0–2.2 (m, 2H, $C\underline{H}_2CH_2N^+$), 2.56 (s, 6H, $PyCH_3$), 3.98 (m, 4H, CH_2O), 4.95 (t, 2H, CH_2N^+), 6.94 (t, 4H, ArH), 7.45 (d, 4H, ArH), 7.95 (s, 1H, γ-PyH), 9.15 (s, 2H, α-PyH). FTIR, KBr (cm^{-1}): 3447, 2936, 2872, 1606, 1500, 1474, 1394, 1273, 1248, 1180, 1035, 977, 825, 808, 692, 518.

2.2.3.9. *1-[6-(4′-Propyloxyl-4-biphenylyloxy)decyl]-pyridinium bromide;* $R_1 = O(CH_2)_3H$, $m = 10$, $R_2 = H$; *C3OBpOC10-Py,* ***9***. The reaction was carried out as before, at 80°C for 20 h. The product was recrystallized from ethyl acetate with a small amount of ethanol and dried at 50°C under vacuum. Yield: 72%, white solid, liquid crystalline. ^{1}H NMR (δ, $CDCl_3$): 1.05 (t, 3H, CH_3), 1.2–1.5 (m, 12H, $(C\underline{H}_2)_6CH_2CH_2N^+$), 1.79 (m, 4H, $C\underline{H}_2CH_2O$), 2.03 (p, 2H, $C\underline{H}_2CH_2N^+$), 3.95 (t, 4H, CH_2O), 5.02 (t, 2H, CH_2N^+), 6.94 (d, 4H, ArH), 7.46 (d, 4H, ArH), 8.10 (t, 2H, β-PyH), 8.50 (t, 1H, γ-PyH), 9.48 (d, 2H, α-PyH). FTIR, KBr (cm^{-1}): 3414, 3040, 2930, 2854, 1635, 1607, 1501, 1394, 1273, 1250, 1179, 1075, 977, 825, 808, 774, 683, 594, 517. EA for $C_{30}H_{40}NO_2Br$: calcd H 7.66, C 68.43, N 2.66, Br 15.17; found H 7.57, C 67.97, N 2.67, Br 15.04%.

2.2.3.10. *1-[6-(4′-Propyloxyl-4-biphenylyloxy)decyl]-4-ethylpyridinium bromide;* $R_1 = O(CH_2)_3H$, $m = 10$, $R_2 = 4\text{-}Et$; *C3OBpOC10-(4-Et)Py,* ***10***. The reaction was carried out as before, at 50°C for 30 h. The product was washed with diethyl ether and dried at 50°C under vacuum. Yield: 93%, pale white solid, m.p. 117–119°C. ^{1}H NMR (δ, $CDCl_3$): 1.05 (t, 3H, CH_3), 1.21–1.52 (m, 15H, $(C\underline{H}_2)_6CH_2CH_2N^+$ and $C\underline{H}_3CH_2Py$), 1.82 (m, 4H, $C\underline{H}_2CH_2O$), 2.01 (p, 2H, $C\underline{H}_2CH_2N^+$), 2.92 (q, 2H, CH_2Py), 3.95 (q, 4H, CH_2O), 4.95 (t, 2H, CH_2N^+), 6.94 (d, 4H, ArH), 7.46 (d, 4H, ArH), 7.85 (d, 2H, β-PyH), 9.31 (d, 2H, α-PyH). FTIR, KBr (cm^{-1}): 3423, 3040, 2930, 2854, 1641, 1607, 1501, 1472, 1394, 1273, 1249, 1179, 1048, 977, 825, 808, 593, 518.

2.2.3.11. *1-[6-(4′-Propyloxyl-4-biphenylyloxy)decyl]-2-ethylpyridinium bromide;* $R_1 = O(CH_2)_3H$, $m = 10$, $R_2 = 2\text{-}Et$; *C3OBpOC10-(2-Et)Py,* ***11***. The reaction was carried out as before, at 60°C for 10 days. Even after ten days of reaction, the bromo-substituted compound could still be detected by TLC. The reaction mixture was washed with cold diethyl ether and dried. The crude product was extracted with hexane to remove the unreacted bromo-substituted compound and finally dried at 50°C under vacuum. Yield: 69%, pale white solid, m.p. 139–141°C. ^{1}H NMR (δ, $CDCl_3$): 1.05 (t, 3H, CH_3), 1.21–1.58 (m, 15H, $(C\underline{H}_2)_6CH_2CH_2N^+$ and $C\underline{H}_3CH_2Py$), 1.82 (m, 4H, $C\underline{H}_2CH_2O$), 2.05 (p, 2H, $C\underline{H}_2CH_2N^+$), 3.18 (q, 2H, CH_2Py), 3.96 (q, 4H, CH_2O), 4.94 (t, 2H, CH_2N^+), 6.96 (d, 4H, ArH), 7.46 (d, 4H, ArH), 7.90 (d, 1H, β-PyH), 8.05 (t, 1H, β-PyH), 8.44 (t, 1H, γ-PyH), 9.81 (d, 1H, α-PyH). FTIR, KBr (cm^{-1}): 3423, 3040, 2930, 2854, 1629, 1607, 1501, 1473, 1394, 1272, 1249, 1179, 1048, 1035, 978, 824, 808, 595, 517.

2.2.3.12. *1-[6-(4′-Propyloxyl-4-biphenylyloxy)decyl]-3,5-dimethylpyridinium bromide;* $R_1 = O(CH_2)_3H$, $m = 10$, $R_2 = 3,5\text{-}Me$; *C3OBpOC10-(3,5-Me)Py,* ***12***. The reaction was carried out as before, at 50°C for 40 h. The product was washed with diethyl ether and dried at 50°C under vacuum. It was recrystallized from ethyl acetate with a small amount of ethanol and dried at 50°C under vacuum. Yield: 97%, white solid, m.p. 130–131°C. ^{1}H NMR (δ, $CDCl_3$): 1.06 (t, 3H, CH_3), 1.2–1.5 (m, 12H, $(C\underline{H}_2)_6CH_2CH_2N^+$), 1.7–1.9 (m, 4H, $C\underline{H}_2CH_2O$), 2.05 (p, 2H, $C\underline{H}_2CH_2N^+$), 2.61 (s, 6H, CH_3Py), 3.98 (q, 4H, CH_2O), 4.90 (t, 2H, CH_2N^+), 6.94 (d, 4H, ArH), 7.48 (d, 4H, ArH), 7.98 (s, 1H, γ-PyH), 9.12 (s, 2H, α-PyH). FTIR, KBr (cm^{-1}): 3417, 2928, 2854, 1607, 1568, 1501, 1472, 1393, 1328, 1273, 1249, 1180, 1137, 1048, 977, 825, 808, 690, 595, 517.

2.2.3.13. *1-[6-(4′-Decyloxyl-4-biphenylyloxy)decyl]-pyridinium bromide;* $R_1 = O(CH_2)_{10}H$, $m = 10$, $R_2 = H$; *C10OBpOC10-Py,* ***13***. The reaction was carried out as before, at 50°C for 25 h. The reaction mixture was precipitated and washed with cold diethyl ether. The crude product was purified by recrystallization from a small amount of EtOH and dried at room temperature under vacuum. Yield: 68%, white solid, liquid crystalline compound. ^{1}H NMR (δ, $CDCl_3$): 0.88 (t, 3H, CH_3), 1.2–1.5 (m, 26H, $CH_3(C\underline{H}_2)_7$ and $(C\underline{H}_2)_6CH_2CH_2N^+$), 1.78 (m, 4H, $C\underline{H}_2CH_2O$), 2.05 (m, 2H, $C\underline{H}_2CH_2N^+$), 3.98 (t, 4H, CH_2O), 5.04 (t, 2H, CH_2N^+), 6.94 (d, 4H, ArH), 7.45 (d, 4H, ArH), 8.08 (t, 2H, β-PyH), 8.46 (t, 1H, γ-PyH), 9.46 (d, 2H, α-PyH). FTIR, KBr (cm^{-1}): 3421, 3038, 2920, 2852, 1633, 1607, 1500, 1475, 1394, 1273, 1249, 1177, 1035, 1011, 995, 824, 808, 777, 722, 688, 595, 518. EA for $C_{37}H_{54}NO_2Br$: calcd H 8.71, C 71.13, N 2.24, Br 12.79; found H 8.63, C 71.03, N 2.01, Br 12.43%.

2.2.3.14. *1-[6-(4′-Decyloxyl-4-biphenylyloxy)decyl]-4-ethylpyridinium bromide; $R_1 = O(CH_2)_{10}H$, $m = 10$, $R_2 = 4$-Et; C10OBpOC10-(4-Et)Py,* ***14***. The reaction was carried out as before, at 50°C for 44 h. The crude product was dissolved in 10 ml of ethanol and filtrated. The clear filtrate was concentrated; the product was precipitated by 30 ml of cold diethyl ether and finally dried at 50°C under vacuum. Yield: 62%, pale white solid, liquid crystalline compound. ^{1}H NMR (δ, $CDCl_3$): 0.90 (t, 3H, CH_3), 1.2–1.5 (m, 29H, $CH_3(C\underline{H}_2)_7$, $(C\underline{H}_2)_6CH_2CH_2N^+$) and $C\underline{H}_3CH_2Py$), 1.77 (m, 4H, $C\underline{H}_2CH_2O$), 2.05 (m, 2H, $C\underline{H}_2CH_2N^+$), 2.92 (q, 2H, $CH_2C\underline{H}_2Py$), 3.98 (t, 4H, CH_2O), 5.04 (t, 2H, CH_2N^+), 6.94 (d, 4H, ArH), 7.45 (d, 4H, ArH), 7.82 (d, 2H, β-PyH), 9.32 (d, 2H, α-PyH). FTIR, KBr (cm^{-1}): 3425, 2920, 2851, 1640, 1607, 1569, 1273, 1248, 1177, 1035, 1013, 996, 850, 823, 808, 722, 595, 518. EA for $C_{39}H_{58}NO_2Br$: calcd H 8.96, C 71.76, N 2.15, Br 12.24; found H 8.81, C 70.03, N 2.13, Br 11.87%.

2.2.3.15. *1-[6-(4′-Decyloxyl-4-biphenylyloxy)decyl]-2-ethylpyridinium bromide; $R_1 = O(CH_2)_{10}H$, $m = 10$, $R_2 = 2$-Et; C10OBpOC10-(2-Et)Py,* ***15***. The reaction was carried out as before, at 50°C for 6 days. The mixture was dissolved in methanol, filtered to obtain a clear solution, and precipitated with cold diethyl ether. The precipitation was repeated twice and the product dried at 50°C under vacuum. Yield: 62%, pale white solid, liquid crystalline compound. ^{1}H NMR (δ, $CDCl_3$): 0.88 (t, 3H, CH_3), 1.2–1.4 (m, 20H, $CH_3(C\underline{H}_2)_6$ and $(C\underline{H}_2)_4CH_2CH_2CH_2N^+$), 1.4–1.65 (m, 7H, $C\underline{H}_2CH_2CH_2O$ and $C\underline{H}_3CH_2Py$), 1.77 (m, 4H, $C\underline{H}_2CH_2O$), 1.98 (m, 2H, $C\underline{H}_2CH_2N^+$), 3.18 (q, 2H, $CH_2C\underline{H}_2Py$), 3.98 (t, 4H, CH_2O), 5.04 (t, 2H, CH_2N^+), 6.94 (d, 4H, ArH), 7.45 (d, 4H, ArH), 7.82 (d, 1H, β-PyH), 8.01 (d, 1H, β-PyH), 8.37 (t, 1H, γ-PyH), 9.90 (d, 1H, α-PyH). FTIR, KBr (cm^{-1}): 3423, 3039, 2921, 2852, 1629, 1608, 1501, 1475, 1394, 1273, 1248, 1177, 1037, 1012, 996, 825, 808, 723, 595, 516. EA for $C_{39}H_{58}NO_2Br$: calcd H 8.96, C 71.76, N 2.15, Br 12.24; found H 8.67, C 70.97, N 2.01, Br 11.93%.

2.2.3.16. *1-[6-(4′-Decyloxyl-4-biphenylyloxy)decyl]-3,5-dimethylpyridinium bromide; $R_1 = O(CH_2)_{10}H$, $m = 10$, $R_2 = 3,5$-Me; C10OBpOC10-(3,5-Me)Py,* ***16***. The reaction was carried out as before, at 50°C for 20 h. The reaction mixture was washed with cold diethyl ether and dried at 50°C under vacuum. Yield: 83%, fine white powder, m.p. 143–144°C. ^{1}H NMR (δ, $CDCl_3$): 0.88 (t, 3H, CH_3), 1.2–1.55 (m, 26H, $CH_3(C\underline{H}_2)_7$ and $(C\underline{H}_2)_6CH_2CH_2N^+$), 1.78 (m, 4H, $C\underline{H}_2CH_2O$), 2.05 (m, 2H, $C\underline{H}_2CH_2N^+$), 2.61 (s, 6H, CH_3Py), 3.98 (t, 4H, CH_2O), 4.89 (t, 2H, CH_2N^+), 6.94 (d, 4H, ArH), 7.45 (d, 4H, ArH), 7.95 (s, 1H, γ-PyH), 9.12 (s, 2H, α-PyH). FTIR, KBr (cm^{-1}): 3431, 2921, 2852, 1607, 1501, 1475, 1394, 1273, 1248, 1178, 1035, 1013, 996, 824, 809, 690, 595, 517.

3. Results and discussion

3.1. *Quaternization*

The quaternization was carried out using the relevant pyridine derivative both as reactant and solvent, because the different compounds are quite soluble in this reaction media, and so the reaction can occur homogeneously. The quaternization of pyridine, 4-ethylpyridine and 3,5-dimethylpyridine was complete within 24–48 hours at 50°C (monitored by TLC). However, with 2-ethylpyridine the reaction was much slower and was not complete in a reasonable time, apparently due to the 2-position being sterically hindered by the ethyl group adjacent to the reaction centre.

3.2. *Phase behaviour*

As shown in table 1, all salts obtained from unsubstituted pyridine, **1**, **5**, **9**, **13**, are liquid crystalline, while all those from 3,5-dimethylpyridine, **4**, **8**, **12**, **16**, are not. With respect to 4-ethylpyridine and 2-ethylpyridine, only those (**14**, **15**) with two decyloxy chains, ($R_1 = O(CH_2)_{10}H$, $m = 10$) exhibit mesophases. The thermal behaviour and the mesophase structure were studied by polarizing optical microscopy (POM), thermogravimetric analysis (TGA), differential scanning calorimetry (DSC) and X-ray diffraction (XRD).

CNBpOC6-Py **1** shows a melting point at 147.5°C in DSC measurements. The melting point can be detected only on first heating because no recrystallization occurs on cooling. Thus, under POM, on cooling from the isotropic phase, only a mesophase can be observed, which is frozen-in at room temperature below its glass transition. The second heating reveals first the glass transition, and then the clearing temperature at 65°C (scheme 2, figure 1). Hence, the mesophase is 'pseudo-monotropic', i.e. is monotropic only with respect to the 'virgin' crystalline phase. TGA measurements reveal the onset of degradation to be at 213°C, i.e. far above all other measurements performed. XRD indicates a smectic A phase with a layer constant c of 27.0 Å at 45°C (table 2). The ratio of the layer constant to the molecular length is $c/L = 1.16$.

C3OBpOC6-Py **5** exhibits in DSC measurements a melting point at 150.5°C and a clearing temperature at 159°C (figure 1). Under POM the mesophase is characterized by a bâtonnet texture with large homeotropic domains, typical for a SmA phase, see figure 2(*a*). TGA measurements reveal the onset of degradation to be at 204°C, i.e. far above all other measurements performed. X-ray measurements indicate a layer spacing of 35.9 Å with a c/L ratio of 1.34 (table 2), which gives evidence for a bilayer arrangement.

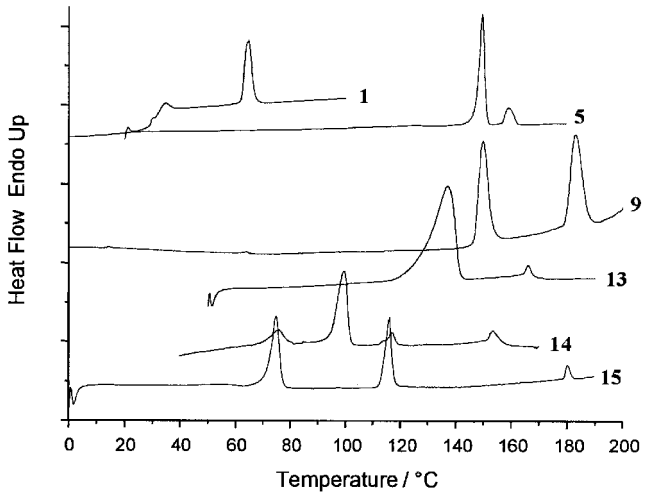

Figure 1. DSC curves for the liquid crystalline pyridinium salts: second heating, scan rates 10 K min^{-1}.

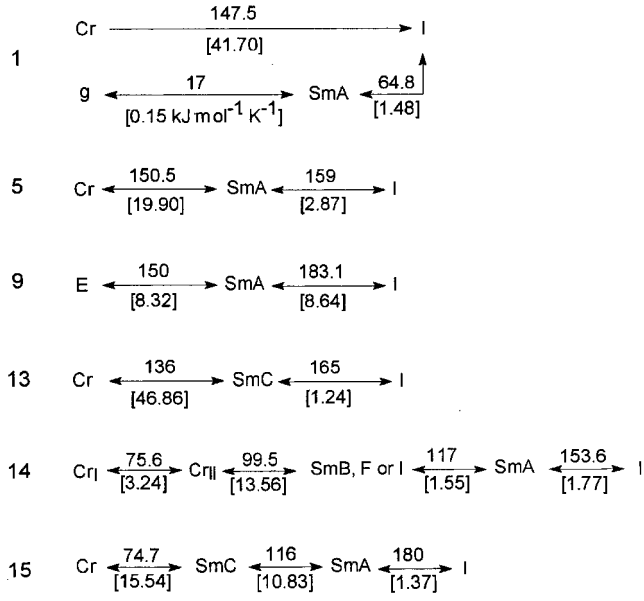

Scheme 2. Polymorphism of the liquid crystalline pyridinium salts: transition temperatures/°C, [ΔH values/kJ mol^{-1}].

C3OBpOC10-Py **9** shows using TGA an onset of degradation at 213°C, i.e. far above all other measurements performed. In DSC on first heating, only two mesophase transitions without any melting were observed. On second heating, a transition from the first to the second mesophase occurs at 150°C with a subsequent clearing peak at 183°C (figure 1). On subsequent cooling, the high temperature mesophase exhibits a focal-conic fan-shaped texture under POM, see figure 2 (*b*). At the transition to the low temperature mesophase, concentric arcs appear across the focal-conic fans, which persist over the whole temperature range of this mesophase. However, cooling from homeotropic domains, a platelet texture can be observed, see figure 2 (*c*). With respect to the texture, the high temperature mesophase may be assigned as a SmA phase, and the low temperature one as an E phase [67]. For the latter, X-ray measurements confirm these results showing two Bragg reflections around $\theta = 9.76°$ (4.54 Å) and 11.12° (3.99 Å), as shown in figure 3 (*a*). These reflections are due to a well developed two-dimensional ordering of molecules within the smectic layers and can be easily indexed as d_{110} and d_{200} reflections of a two-dimensional centered rectangular lattice. The rectangular cell parameters $a = 7.98$ Å and $b = 5.52$ Å are very close to those of other E phases

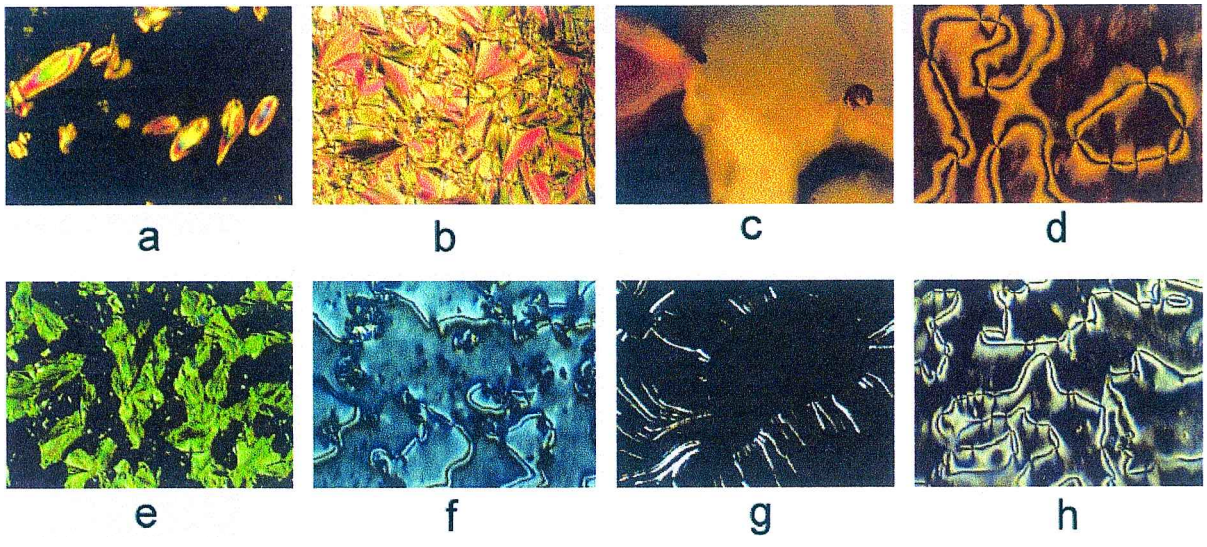

Figure 2. Textures of the liquid crystalline pyridinium salts: (*a*) **5**, on cooling, at 145°C, ×400; (*b*) **9**, on cooling, at 153°C, ×200; (*c*) **9**, on cooling, at 145°C, ×100; (*d*) **13**, on cooling, at 148°C, ×200; (*e*) **14**, on cooling, at 144°C, ×100; (*f*) **14**, on cooling, at 117°C, ×200; (*g*) **15**, on cooling, at 128°C, ×100; (*h*) **15**, on cooling, at 118°C, ×200.

Table 2. Structural data for the LC pyridinium salts.

No.	Pyridinium derivative	Molecular length L/Å[a]	T/°C	θ/°	d_{hkl}/Å	$h\,k\,l$	Lattice constants/Å[b]	Mesophase	c/L
1	CNBpOC6-Py	23.3	45	1.63	27.08	0 0 1	$c = 27.0$	SmA	1.16
				3.27	13.5	0 0 2			
				10.66	4.16	halo			
5	C3OBpOC6-Py	26.3	150	1.23	35.90		$c = 35.9$	SmA	1.34
				10.34	4.29				
9	C3OBpOC10-Py	31.5	155	1.22	36.18	0 0 1	$c = 36.3$	SmA	1.15
				2.45	18.17	0 0 2			
				9,81	4.52	halo			
			120	1.22	36.18	0 0 1	$c = 36.2$	E	1.15
				2.45	18.17	0 0 2			
				4.89	9.04	0 0 4			
				9.76	4.54	1 1 0	$a = 7.98$		
				11.12	3.99	2 0 0	$b = 5.52$		
13	C10OBpOC10-Py	39.1	150	0.71	62.16	0 0 1	$c = 62.1$	SmC	1.59
				1.43	30.86	0 0 2			
				2.12	20.82	0 0 3			
				2.85	15.49	0 0 4			
				9.93	4.47	halo			
14	C10OBpOC10-(4-Et)Py	42.3	140	0.71	62.16	0 0 1	$c = 63.5$	SmA	1.50
				1.38	31.98	0 0 2			
				2.06	21.43	0 0 3			
				9.98	4.45	halo			
			105	0.68	64.9	0 0 1	$c = 66.2$	SmB, F or I	1.57
				1.35	32.7	0 0 2			
				1.98	22.29	0 0 3			
				3.28	13.46	0 0 5			
				3.97	11.13	0 0 6			
				9.82	4.52	halo			
				10.71	4.15				
15	C10OBpOC10-(2-Et)Py	39.1	140	0.69	63.96	0 0 1	$c = 63.7$	SmA	1.63
				1.39	31.75	0 0 2			
				2.08	21.22	0 0 3			
				9.75	4.55	halo			
			100	0.63	70.06	0 0 1	$c = 69.2$	SmC	1.77
				1.28	34.48	0 0 2			
				1.93	22.87	0 0 3			
				10.01	4.43	halo			

[a] L was calculated for extended alkyl chains with the computer programme Alchemy 2000, Tripos Inc., St. Louis, USA.
[b] The lattice constant c (layer spacing d) was calculated as an average value of n reflections d_{hkl}, according to $c = (\Sigma_1^n 1 \times d_{hkl})/n$

[68, 69]. The smectic A phase XRD pattern shows an inverse intensity, i.e. the intensity of the third order reflection is stronger than that of the second one, figure 3(*a*). In addition, the enthalpy ($8.63\,\mathrm{kJ\,mol^{-1}}$) associated with isotropization is relatively large with respect to literature values for smectic A–isotropic enthalpies (4–6 $\mathrm{kJ\,mol^{-1}}$) (scheme 2). This may be caused by the breakdown of the order in systems having strong interactions such as hydrogen bonding or, in our case, ionic forces.

C10OBpOC10-Py **13** shows in DSC measurements one large melting transition at 136°C and a small mesophase to isotropic transition at 165°C (figure 1). TGA measurements reveal the onset of the degradation to be at 205°C, i.e. far above all other measurements performed. Under the POM, homeotropic alignment was usually observed for the mesophase between 136 and 165°C, although some bright lines could be observed upon shearing, which shrank and returned to the homeotropic state upon relaxation. A schlieren texture, as shown in figure 2, was obtained by using a glass plate as purchased without further cleaning. In accordance with these observations, and taken together with the XRD data (table 2), C10OBpOC10-Py **13** is considered to show a SmC phase between 136 and 165°C.

TGA of C10OBpOC10-(4-Et)Py **14** shows the onset of the degradation to be at 203°C, i.e. far above all other measurements performed. DSC measurements (figure 1)

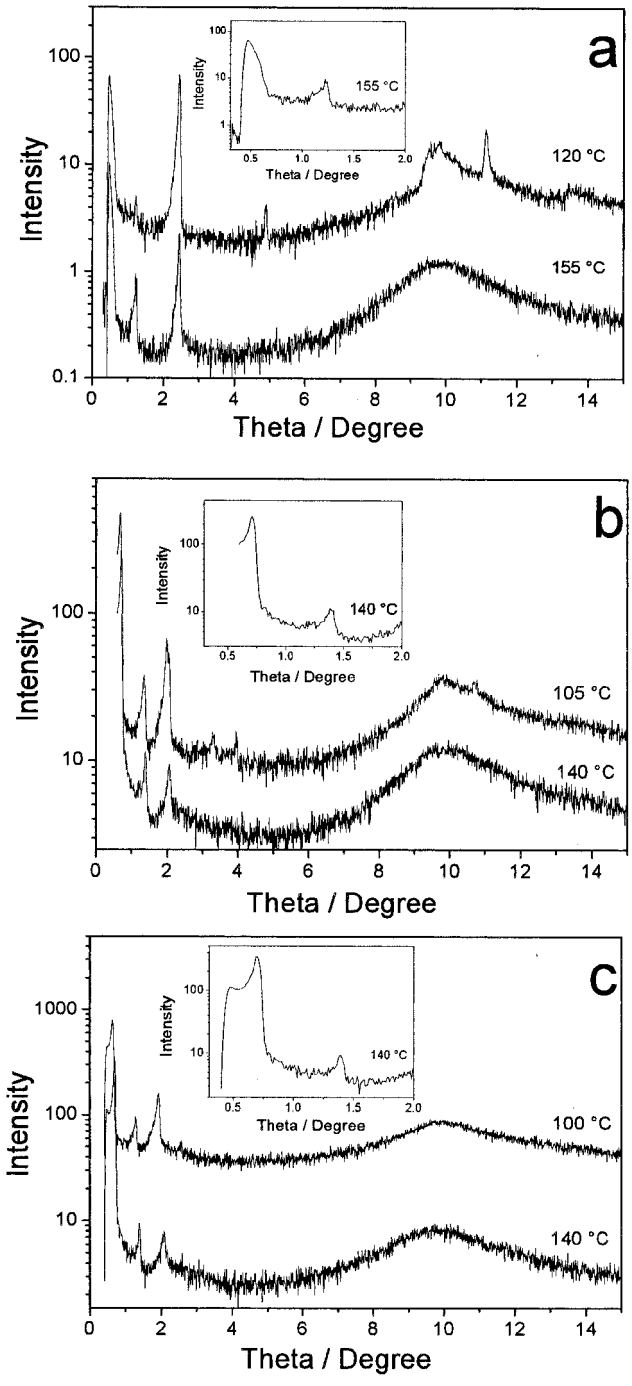

Figure 3. Representative XRD patterns of the liquid crystalline pyridinium salts: (*a*) C3OBpOC10-Py **9** (the signal around 0.5° is not a peak, but the primary beam edge); (*b*) C10OBpOC10-(4-Et)Py **14**; (*c*) C10OBpOC10-(2-Et)Py **15**.

reveal a crystal–crystal transition at 75.5°C, a melting to a first mesophase at 99.5°C, a transition to a second mesophase at 117°C and clearing at 153.5°C, and in accord with observations made using POM. On cooling from the isotropic phase into the high temperature mesophase, first a texture containing bâtonnets and later a focal-conic fan-like texture was observed together with a strong tendency to form homeotropic domains. These observations indicate a SmA phase. This assignment is confirmed by XRD which gives sharp 0 0 1, 0 0 2 and 0 0 3 reflections at $\theta = 0.71°$, 1.38° and 2.06° (62.16, 31.98 and 21.43 Å) and a halo at 9.98° (4.45 Å), see figure 3(*b*) and table 2. For the highly ordered mesophase observed at lower temperature, up to the sixth order reflection can be observed. The wide angle reflections around 9.82° (4.52 Å) and 10.71° (4.15 Å) indicate that the molecules exhibit positional ordering within a layer. From the schlieren texture observed, this smectic phase could be a SmB, SmF or SmI phase [70].

For C10OBpOC10-(2-Et)Py **15**, TGA measurements reveal the onset of the degradation to be at 193°C, i.e. far above all other measurements performed. DSC measurements show a melting point at 75°C, two mesophases with a transition at 116°C and a clearing temperature at 180°C (figure 1). As revealed by POM, a strong tendency to form homeotropic alignment with only a transient focal-conic texture was observed for the high temperature mesophase. The XRD pattern at 140°C confirm a SmA phase and contains 0 0 1, 0 0 2 and 0 0 3 reflections at $\theta = 0.69°$, 1.39° and 2.08° (63.96, 31.75 and 21.22 Å) with a lattice constant *c* (layer distance *d*) of 63.7 Å and a halo at 9.75° (4.55 Å); see figure 3(*c*) and table 2. On cooling from the homeotropic domains of the SmA phase, a typical schlieren texture with four brushes can be observed as shown in figure 2(*b*). From this, we conclude that a SmC phase appears at lower temperatures. XRD at 100°C shows 0 0 1, 0 0 2 and 0 0 3 reflections at $\theta = 0.63°$, 1.28° and 1.93° (70.06, 34.48 and 22.87 Å) with $c = 69.2$ Å and a halo at 10.01° (4.43 Å); see figure 3(*c*) and table 2. We propose that the observed unusual increase in the lattice constant *c* (layer distance *d*) on going from the SmA to the SmC phase may be accounted for in terms of both, the reduced conformational changes in the two decyl chains per molecule and the reduced interdigitation and mobility in the ionic region of the bilayers present (see later).

The polymorphism of all the liquid crystalline compounds is shown in scheme 2.

3.3. *Structure of the smectic A mesophases*

All the compounds exhibit smectic mesophases, as do other liquid crystals of the pyridinium type [37–50]. Furthermore, the SmA phases show a strong tendency to form homeotropic alignment as observed under POM; the ionic structure obviously favours this behaviour. In order to analyse the SmA structures, the lattice constants *c* (layer distance *d*) were compared with the molecular length *L*, calculated for extended molecular chains by computer simulation (Alchemy 2000, Tripos, Inc,

St. Louis, USA). To explain the different *c*/*L* ratios for the different pyridinium salts (see table 2), three different arrangements are proposed for the SmA layer structures.

It is well known that smectogens containing terminal cyano groups form pairwise antiparallel associations of their polar aromatic cores to compensate for their dipole moments. As a result, in the case of 4-alkoxy- and 4-alkyl-4′-cyanobiphenyls, the average lamellar spacing corresponds to 1.4 times the molecular length [71, 72], and similar values are known for other terminal cyano group-containing systems. However, for CNBpOC6Py **1** we observe a *c*/*L* ratio of 1.16, i.e. a layer spacing slightly greater than the length of one molecule. Apparently, a dimeric head-to-head association of the cyanobiphenyl groups with a resulting large layer spacing does not occur, because of the presence of the ionic pyridinium moieties and their bromide counterions. We propose nevertheless an antiparallel arrangement of the molecules, but now with head-to-tail interdigitation as shown in figure 4(*a*). In this model, the polar cyano group and the ionic moiety stabilize each other by forming a polar array, separated from the apolar alkyl chains and biphenyl cores. A smectic A phase with a layer spacing slightly larger than the molecular length was termed SmA_1, indicating that its layer structure is more than a simple packing of single molecules [73].

The latter arrangement seems to be realized for the SmA phase of C3OBpOC6-Py **5** and C3OBpOC10-Py **9**, where instead of a cyano group a short propyloxy group is attached to the biphenyl core. Here, the necessity of forming a head-to-tail structure is no longer present because of the absence of polar head groups. Thus, a head-to-head arrangement should result in a layer distance slightly longer than the molecular length, presumably because of the presence of the bromide anions, see figure 4(*b*). The stronger intensity of the third order reflection and the high clearing enthalpy (both described earlier) could be an indication of a relatively high degree of ordering of the ionic species in their sub-region.

For compounds C10OBpOC10-(4-Et)Py **14** and C10OBpOC10-(2-Et)Py **15**, the layer spacing of the SmA structures is larger than the calculated molecular lengths. This can be explained by the occurrence of an interdigitated head-to-head bilayer structure, see figure 4(*c*). Thus, the phase structure of the ionic liquid crystals studied, having long terminal alkyl chains corresponds to a SmA_d phase [73].

The observation in § 3.2 that for compound **15** the layer spacing of the SmC phase is larger than that of the SmA phase is presumably also related to the specific bilayer arrangement (figure 4) of the SmC phase: now we have tilted biphenyl cores (sublayers A), decyl chains (sublayers B) and the ionic pyridinium region (sublayer C). Usually in the SmC phases, a tilt of the cores with respect to the layer normal leads to smaller layer spacings. In our case this should likewise be valid for the dimensions of the two sublayers A in the bilayer. However, at lower temperatures the reduced conformational mobility (decrease of *gauche* conformations with decreasing temperature) of the decyl chains should lead to an increase in the thickness of all four sublayers B in the bilayer, which may already more than compensate for the shrinking of the two sublayers A. A similar effect has recently been described in the literature [74]. A further contribution to the remarkably larger overall layer spacing in the SmC phase may possibly be from a higher degree of order, i.e. a shorter interdigitation length in the ionic sublayer C.

4. Conclusion

We have shown that pyridinium moieties linked to a rod-like biphenyl core via ω-substituted alkyl spacers can form ionic liquid crystals. Unsubstituted pyridinium groups promote mesomorphism; 2- and 4-ethyl-substituted pyridinium groups form liquid crystalline phases only with sufficiently long alkyl chains, i.e. decyl chains on both sides of the biphenyl core. 3,5-Dimethyl substitution hinders mesophase formation.

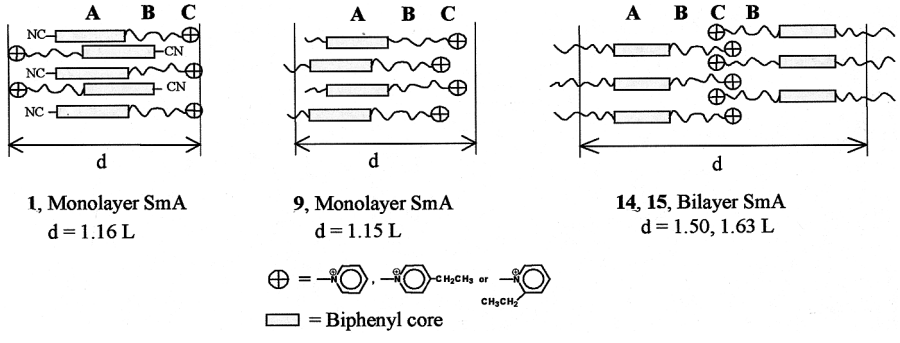

Figure 4. Proposed SmA mesophase structures of ABC types: layer distance *d* = lattice constant *c*; *L* = calculated molecular length.

The substitution pattern at the pyridinium groups influences the formation of different types of smectic phases, as can be seen in compounds **13**, **14** and **15**. Similarly the length of the alkyl chains influences the polymorphism of the smectic phases as can be shown by the additional appearance of the E phase in compound **13** with respect to **5** and **9**.

In principle, the different smectic A structures consist, in all cases, of different sublayers A of the biphenyl rods, sublayers B of the flexible alkyl chains and polar or ionic sublayers C containing the pyridinium and bromide ions (for compound **1** together with the cyano groups), i.e. are of an 'ABC-type structure'. This specific architecture and the ionic character of the system can explain the unusual increase of the layer spacing in the SmC phase with respect to that of the SmA phase for compound **15**.

The following financial support is gratefully acknowledged by the authors: V. S. to TEMPUS project JEP 12387-98, L. C. to Deutsche Sonderforschungsgemeinschaft, SFB 481, project A4.

References

[1] Neve, F., 1996, *Adv. Mater.*, **8,** 277.
[2] Oriol, L., 1996, in *Metallomesogens*, edited by J. L. Serrano (Weinheim: Wiley-VCH), p. 227.
[3] Ros, R. B., 1996, in *Metallomesogens*, edited by J. L. Serrano (Weinheim: Wiley-VCH), p. 471.
[4] Van Nostrum, C. F., 1996, *Adv. Mater.*, **8,** 1027.
[5] Mukkumala, R., Burns, C. L., Catchings, R. M., and Weiss, R. G., 1996, *J. Am. chem. Soc.*, **118,** 9498 and references therein.
[6] Kansui, H., Hiraoka, S., and Kunieda, T., 1996, *J. Am. chem. Soc.*, **118,** 5346 and references therein.
[7] Serrano, L. J (editor), 1996, *Metallomesogens* (Weinheim: Wiley-VCH).
[8] Donnio, B., and Bruce, D. W., 1999, in *Structure and Bonding*, Vol. 95, edited by D. M. P. Mingos (Berlin: Springer Verlag), Liquid Crystals II, pp. 194–247.
[9] Busico, V., Castaldo, D., and Vacatello, M., 1981, *Mol. Cryst. liq. Cryst.*, **78,** 221.
[10] Dalcanale, E., 1996, *Compr. supramol. Chem.*, **10,** 583.
[11] Liebmann, A., Mertesdorf, C., Plesnivy, T., Ringsdorf, H., and Wendorff, J. H., 1991, *Angew. Chem., int. Ed. Engl.*, **30,** 1375; Liebmann, A., Mertesdorf, C., Plesnivy, T., Ringsdorf, H., and Wendorff, J. H., 1991, *Angew. Chem.*, **103,** 1358.
[12] Lattermann, G., Schmidt, S., Kleppinger, R., and Wendorff, J. H., 1992, *Adv. Mater.*, **4,** 30.
[13] Walf, G. H., Benda, R., Litterst, F. J., Stebani, U., Schmidt, S., and Lattermann, G., 1998, *Chem. Eur. J.*, **4,** 93.
[14] Facher, A., Lattermann, G., Domracheva, N., and Ovchinnikov, I. (in preparation).
[15] Serrano, J. L., and Sierra, T., 1996, in *Metallomesogens*, edited by J. L. Serrano (Weinheim: Wiley-VCH), p. 51.
[16] Fischer, H., Plesnivy, T., Ringsdorf, H., and Seitz, M., 1998, *J. mater. Chem.*, **8,** 343.
[17] Stebani, U., 1995, PhD thesis (Bayreuth), pp. 115–122.
[18] Stebani, U., Lattermann, G., Wittenberg, M., and Wendorff, J. H., 1996, *Angew. Chem., int. Ed. Engl.*, **35,** 1858; Stebani, U., Lattermann, G., Wittenberg, M., and Wendorff, J. H., 1996, *Angew. Chem.*, **108,** 1941.
[19] Facher, A., 2000, PhD thesis (Bayreuth), pp. 165–195.
[20] Serrano, J. L., and Sierra, T., 1996, in *Metallomesogens*, edited by J. L. Serrano (Weinheim: Wiley-VCH), p. 46.
[21] Bruce, D. W., Dunmur, D. A., Lalinde, E., and Styring, P., 1986, *Nature*, **323,** 791.
[22] Marcos, M., Ros, M. B., Serrano, J. L., Esteruelas, M. A., Sola, E., Oro, L. A., and Barbera, J., 1990, *Chem. Mater.*, **2,** 748.
[23] Busico, V., Corradini, P., and Vacatello, M., 1983, *J. phys. Chem.*, **87,** 1631 and references therein.
[24] Paleos, C. M., Margomenou-Leonidopoulou, G., and Malliaris, A., 1988, *Mol. Cryst. liq. Cryst.*, **161,** 385 and references therein.
[25] Sellens, R. J., Runciman, P. J. I., Griffin, A. C., and Bryant, E. S., 1989, *Mol. Cryst. liq. Cryst.*, **166,** 123.
[26] Matsunaga, Y., and Tsujimura, T., 1994, *Mol. Cryst. liq. Cryst.*, **250,** 161 and references therein.
[27] Kawamata, J., Matsunaga, Y., and Ohtsu, K., 1994, *Mol. Cryst. liq. Cryst.*, **257,** 27 and references therein.
[28] Ujiie, S., and Iimura, K., 1994, *Chem. Lett.*, 17.
[29] Paleos, C., Arkas, M., Segrouchni, R., and Skoulios, A., 1995, *Mol. Cryst. liq. Cryst.*, **268,** 179 and references therein.
[30] Tsiourvas, D., Paleos, C. M., and Skoulios, A., 1999, *Liq. Cryst.*, **26,** 953 and references therein.
[31] Stebani, U., and Lattermann, G., 1995, *Adv. Mater.*, **7,** 578.
[32] Lattermann, G., Schmidt, S., and Gallot, B., 1992, *J. Chem. Soc., chem. Commun.*, 1091.
[33] Zinsou, A., Veber, M., Strezelecka, H., Jallabert, C., and Levelut, A. M., 1994, *Liq. Cryst.*, **17,** 513.
[34] Davidson, P., Jallabert, C., Levelut, A. M., Strezelecka, H., and Veber, M., 1988, *Liq. Cryst.*, **3,** 133 and references therein.
[35] Veber, M., Jallabert, C., Strezelecka, H., Julien, O., and Davidson, P., 1990, *Liq. Cryst.*, **8,** 775.
[36] Veber, M., and Berruyer, G., 2000, *Liq. Cryst.*, **27,** 671 and references therein.
[37] Knight, B. A., and Shaw, B. D., 1938, *J. chem. Soc.*, 682.
[38] Sudhölter, E. J. R., Engberts, J. B. F. N., and de Jeu, W., 1982, *J. phys. Chem.*, **86,** 1908.
[39] Bazuin, C. G., Guillon, D., Skoulios, A., and Nicoud, J. F., 1986, *Liq. Cryst.*, **1,** 181.
[40] Somashekar, R., 1987, *Mol. Cryst. liq. Cryst.*, **146,** 225.
[41] Chachaty, C., Bredel, T., Tistchenko, A. M., Caniparoli, J. P., and Gallot, B., 1988, *Liq. Cryst.*, **3,** 815.
[42] Cheng, P., Subramanyam, S., and Blumstein, A., 1992, *Polym. Prepr.*, **33,** 339.
[43] Nusselder, J. J. H., Engberts, J. B. F. N., and van Doren, H., 1993, *Liq. Cryst.*, **13,** 213.
[44] Cheng, P., Blumstein, A., and Subramanyam, S., 1995, *Mol. Cryst. liq. Cryst.*, **269,** 1.
[45] Kosaka, Y., Kato, T., and Uryu, T., 1995, *Liq. Cryst.*, **18,** 693.
[46] Tabrizian, M., Soldera, A., Couturier, M., and Bazuin, C. G., 1995, *Liq. Cryst.*, **18,** 475.
[47] Haramoto, Y., Ujiie, S., and Nanasawa, M., 1996, *Liq. Cryst.*, **21,** 923.

[48] Haramoto, Y., Akiyama, Y., Segawa, R., Nanasawa, M., Ujiie, S., and Holmes, A. B., 1998, *Liq. Cryst.*, **26,** 1425.
[49] Haramoto, Y., Akiyama, Y., Segawa, R., Ujiie, S., and Nanasawa, M., 1998, *J. mater. Chem.*, **8,** 275.
[50] Haramoto, Y., Kusakabe, Y., Nanasawa, M., Ujiie, S., Mang, S., Moratti, S. C., and Holmes, A. B., 2000, *Liq. Cryst.*, **27,** 262.
[51] Haramoto, Y., Kusakabe, Y., Nanasawa, M., Ujiie, S., Mang, S., Schwarzwalder, C., and Holmes, A. B., 2000, *Liq. Cryst.*, **27,** 1393.
[52] Haramoto, Y., Nanasawa, M., Ujiie, S., and Holmes, A. B., 2000, *Mol. Cryst. liq. Cryst. Sci. Technol. A*, **348,** 129.
[53] Vuillaume, P. Y., Bazuin, C. G., and Galin, J.-C., 2000, *Macromolecules*, **33,** 781.
[54] Gordon, C. M., Holbrey, J. D., Kennedy, A. R., and Seddon, K. R., 1998, *J. mater. Chem.*, **8,** 2627.
[55] Yousif, Y. Z., Kamounah, F. S., Ali, M. K., and Al-Rawi, J. M. A., 1990, *Spectrosc. Lett.*, **23,** 811.
[56] Haramoto, Y., Yin, M., Matukawa, Y., Ujiie, S., and Nanasawa, M., 1995, *Liq. Cryst.*, **19,** 319.
[57] Yousif, Y. Z., Jenkins, A. D., Walton, D. R. M., and Al-Rawi, J. M. A., 1990, *Eur. Polym. J.*, **26,** 901.
[58] Kijima, M., Setoh, K., and Shirakawa, H., 2000, *Chem. Lett.*, 936.
[59] Navarro-Rodriguez, D., Frère, Y., Gramain, P., Guillon, D., and Skoulios, A., 1991, *Liq. Cryst.*, **9,** 321 and references therein.
[60] Hessel, V., Ringsdorf, H., Festag, R., and Wendorff, J. H., 1993, *Makromol. Chem., rapid Commun.*, **14,** 707.
[61] Bravo-Grimaldo, E., Navarro-Rodriguez, D., Skoulios, A., and Guillon, D., 1996, *Liq. Cryst.*, **20,** 393 and references therein.
[62] Chovino, C., Frère, Y., Guillon, D., and Gramain, P., 1997, *J. polym. Sci.*, **27,** 1595.
[63] Bernhardt, H., Weissflog, W., and Kresse, H., 1999, *Mol. Cryst. liq. Cryst.*, **330,** 1451 and references therein.
[64] Bumagin, N. A., and Luzikova, E. V., 1997, *J. organomet. Chem.*, **532,** 271.
[65] Nishikido, J., Inazu, T., and Yoshino, T., 1973, *Bull. chem. Soc. Jpn.*, **46,** 263.
[66] Imrie, C. T., and Luckhurst, G. R., 1998, *J. mater. Chem.*, **8,** 1339.
[67] Goodby, J. W., and Gray, G. W., 1998, in *Handbook of Liquid Crystals*, Vol. 1, edited by D. Demus, J. Goodby, G. W. Gray, H.-W. Spiess and V. Vill (Weinheim: Wiley VCH), pp. 16–23.
[68] Doucet, J., Levelut, A. M., Lambert, M., Liebert, L., and Strzelecki, L., 1975, *J. Phys. Coll. Paris.*, **C1-36,** 13.
[69] Gray, G. W., and Goodby, J. W., 1984, in *Smectic Liquid Crystal Textures and Structures*, edited by L. Hill (Philadelphia: Heyden), p. 82.
[70] Demus, D., and Richter, L., 1978, *Textures of Liquid Crystals* (Weinheim: Verlag-Chemie), p. 100.
[71] Leadbetter, A. J., Durrant, J. L. A., and Rugman, M., 1977, *Mol. Cryst. liq. Cryst. Lett.*, **34,** 231.
[72] Leadbetter, A. J., Frost, J. C., Ganghan, J. P., Gray, G. W., and Mosley, A., 1979, *J. Phys. (Paris)*, **40,** 375.
[73] Cladis, P. E., 1998, in *Handbook of Liquid Crystals*, Vol. 1, edited by D. Demus, J. Goodby, G. W. Gray, H.-W. Spiess and V. Vill (Weinheim: Wiley-VCH), p. 391–405.
[74] Wirth, I., Diele, S., Eremin, A., Pelzl, G., Grand, S., Kovalenko, L., Pancenko, N., and Weissflog, W., 2001, *J. mater. Chem.*, **11,** 1642.